SURFACES, INTERFACES, AND THIN FILMS

Structural Features of Textured Zinc-Oxide Films Obtained by the Ion-Beam Sputtering Method

V. G. Kostishin[a,*], A. Yu. Mironovich[a], A. V. Timofeev[a], I. M. Isaev[a], R. I. Shakirzyanov[a], A. I. Ril[b], and A. A. Sergienko[a]

[a] *National University of Science and Technology "MISiS", Moscow, 119049 Russia*
[b] *Kurnakov Institute of General and Inorganic Chemistry, Russian Academy of Sciences, Moscow, 119991 Russia*
*e-mail: drvgkostishyn@mail.ru

Abstract—Textured ZnO films obtained on amorphous substrates using the ion-beam sputtering method are studied. X-ray diffraction and atomic-force microscopy methods show that the resulting films have a polycrystalline structure immediately after deposition. It is established that further annealing of the samples in the temperature range from 200°C to 500°C results in recrystallization, which leads to changes in the grain size and surface roughness. A dependence of the crystallization intensity on the deposition conditions is found, which is related to the number of defects in the unannealed films. In films with an initially more perfect structure, heat treatment at 500°C results in the growth of grains by more than 2 times and a decrease in the roughness by ~40%.

1. INTRODUCTION

Zinc oxide ZnO and its films as electronic materials are mainly used in various optical devices in the ultraviolet range [1]. However, there are also alternative practical applications. In addition to their direct use in devices, anisotropic ZnO (001) films can be used as buffer layers for films of other materials, such as $BaFe_{12}O_{19}$ (001) hexagonal ferrites [2, 3]. Despite belonging to different spatial symmetry groups, the textured growth of hexaferrite on zinc oxide is determined by the common structure of their oxygen planes. In addition, these planes are characterized by hexagonal dense packing; therefore, ZnO nuclei with the (001) orientation have a minimum surface energy [4], which increases the probability of their formation and opens up the possibility of obtaining a textured film on amorphous substrates. This statement has not only theoretical grounds but is also directly confirmed by the results of experiments [5, 6]. The "amorphous substrate−spontaneous formation of (001) ZnO−pseudomorphic growth of (001) hexaferrite" scheme seems to be a more cost-effective solution than the classical "single-crystal substrate/film" structure. This approach was performed in [7], where $BaFe_{12}O_{19}$ (001)/ZnO (001)/fused quartz films were produced.

This application of anisotropic ZnO films imposes special requirements on their structure. It is important to obtain films with the highest degree of texture, since a deviation in the buffer-layer orientation is inherited by the functional coating; as a result, the parameters of the synthesized material differ from those expected. A high roughness of the buffer layer leads to similar consequences, since nucleation may occur on the side faces of protruding elements of the relief, thus causing the appearance of crystallites of undesirable orientations. The roughness is affected by various factors, such as the annealing conditions. ZnO films are annealed to improve the crystallinity and annihilation of oxygen vacancies. The annealing temperature in different studies varies from 350 to 900°C [5, 6, 8−12]. The presence of such a temperature spread and the emphasis on the temperature dependences of the functional properties of ZnO do not allow one to determine unambiguously the optimal conditions for the production of anisotropic films that are characterized precisely by their perfect texture using published data. Of course, there are studies focused on investigating the structural characteristics of ZnO films [13]. On the other hand, there are few such publications; therefore, it is reasonable to conduct such studies using alternative synthesis conditions which may affect the results.

The objective of this study is to investigate the influence of the annealing temperature on the features of the crystal structure and microrelief of textured
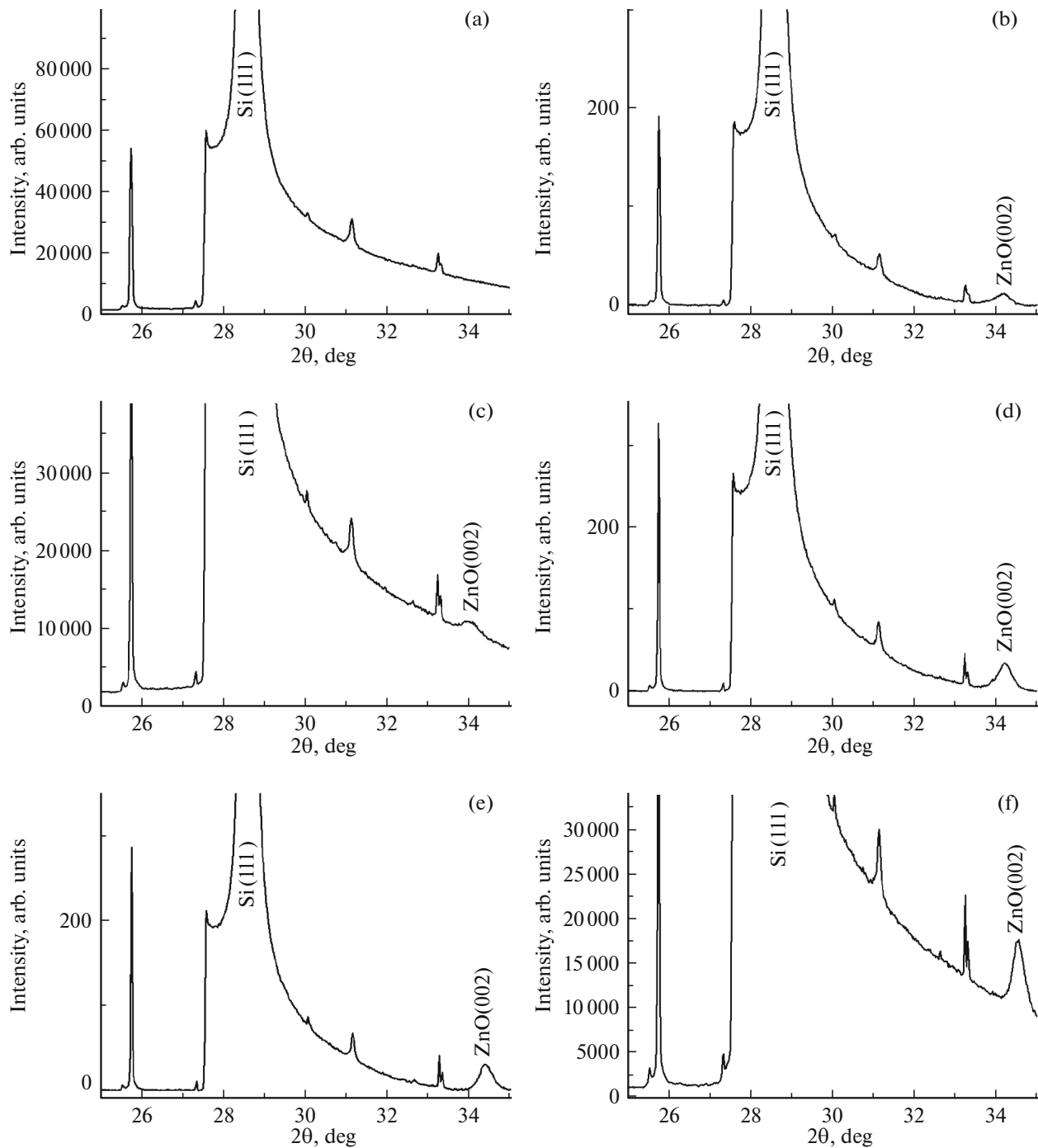
Fig. 1. X-ray diffraction patterns of ZnO films on a SiO$_2$/Si substrate: (a) SiO$_2$/Si substrate without a ZnO film; (b) ZnO film on a SiO$_2$/Si substrate without heat treatment; ZnO film on a SiO$_2$/ Si substrate after annealing at 100 (c), 200 (d), 350 (e), and 500°C (f).

ZnO films obtained on oxidized silicon substrates using the ion-beam sputtering technique.

2. EXPERIMENTAL

Thermally oxidized silicon wafers with the (111) orientation were used as substrates. They were oxi-

dized at a temperature of 1050°C in an atmosphere of nitrogen and oxygen. ZnO films were deposited by the method of ion-beam sputtering of a target that was manufactured by the pressing of a pure-grade ZnO powder (pure for analysis). The substrates were washed for 5 min in methyllirolidone-*N* using an ultrasonic bath. The sputtering process was performed
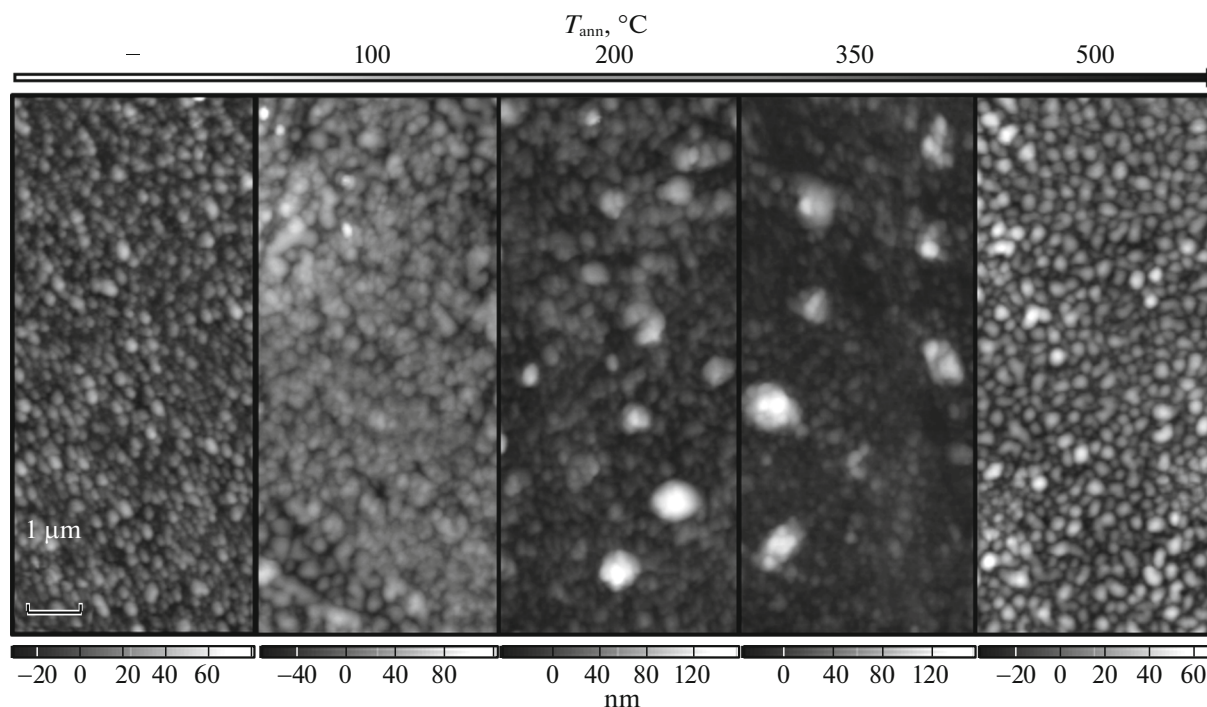
T_{ann}, °C

Fig. 2. AFM images of ZnO films after their annealing at various temperatures.

in a vacuum chamber of the UVN-71-3M apparatus for 7 min. Before the films were deposited, the substrates were heated to 300°C and kept at this temperature for 10 min at a residual pressure in the chamber of $(0.5-1) \times 10^{-2}$ Pa to remove moisture and degas the substrates. Deposition was performed without heating after the substrates were cooled to room temperature. The distance from the target to the substrate was 25, 40, and 45 mm. The discharge current was 40–50 mA, the discharge voltage was 2–2.1 kV, and the working Ar-gas pressure was maintained at a level of $4.5-5 \times 10^{-2}$ Pa. The resulting films were annealed in air at temperatures of 100, 200, 350, and 500°C for 1 h. The thickness of the obtained films was measured using a DekTak 150 contact profilometer. X-ray diffraction patterns (XRDs) were obtained using a BRUKER D8

Fig. 3. Schematic image of different orientations of ZnO crystallites.

ADVANCE diffractometer (CuK_α radiation, $\lambda = 0.154$ nm, $U = 40$ kV, and $I = 40$ mA). Recording was performed in increments of 0.02° in the range $2\theta = 15°-100°$. When processing the XRDs, the ICDD PDF-2 powder diffractometer database and the Diffrac.SuiteEVA software environments were used. Atomic force microscopy (AFM) images were obtained using an NT-MDT NTEGRA Prima scanning probe microscope.

3. RESULTS AND DISCUSSION

The first series of samples was obtained at a target–substrate distance of 25 mm. According to profilometry data, the thickness of all films was 0.2 ± 0.01 µm, which confirms the stability of the deposition process.

The X-ray diffraction patterns for these samples are shown in Fig. 1. The displayed range of values of $2\Theta = 25°-35°$ fully reflects all changes that are observed in the films. In addition to the intense (111) silicon peak, many other reflections are present in all the XRDs. As can be seen in Fig. 1a, almost all of these peaks belong to the substrate and likely demonstrate the presence of SiO_2 crystalline inclusions. Although thermally oxidized silicon is considered to be amorphous in the manufacturing environment, several scientific papers indicate the possibility of the formation of crystalline SiO_2 [14, 15]. In any case, revealing the nature of these reflections is beyond the scope of this study. As for the films themselves, a peak of ~34°–35°, which is identified as ZnO (002), can be distinguished in all the

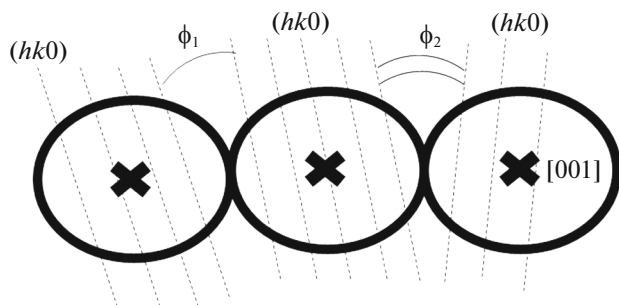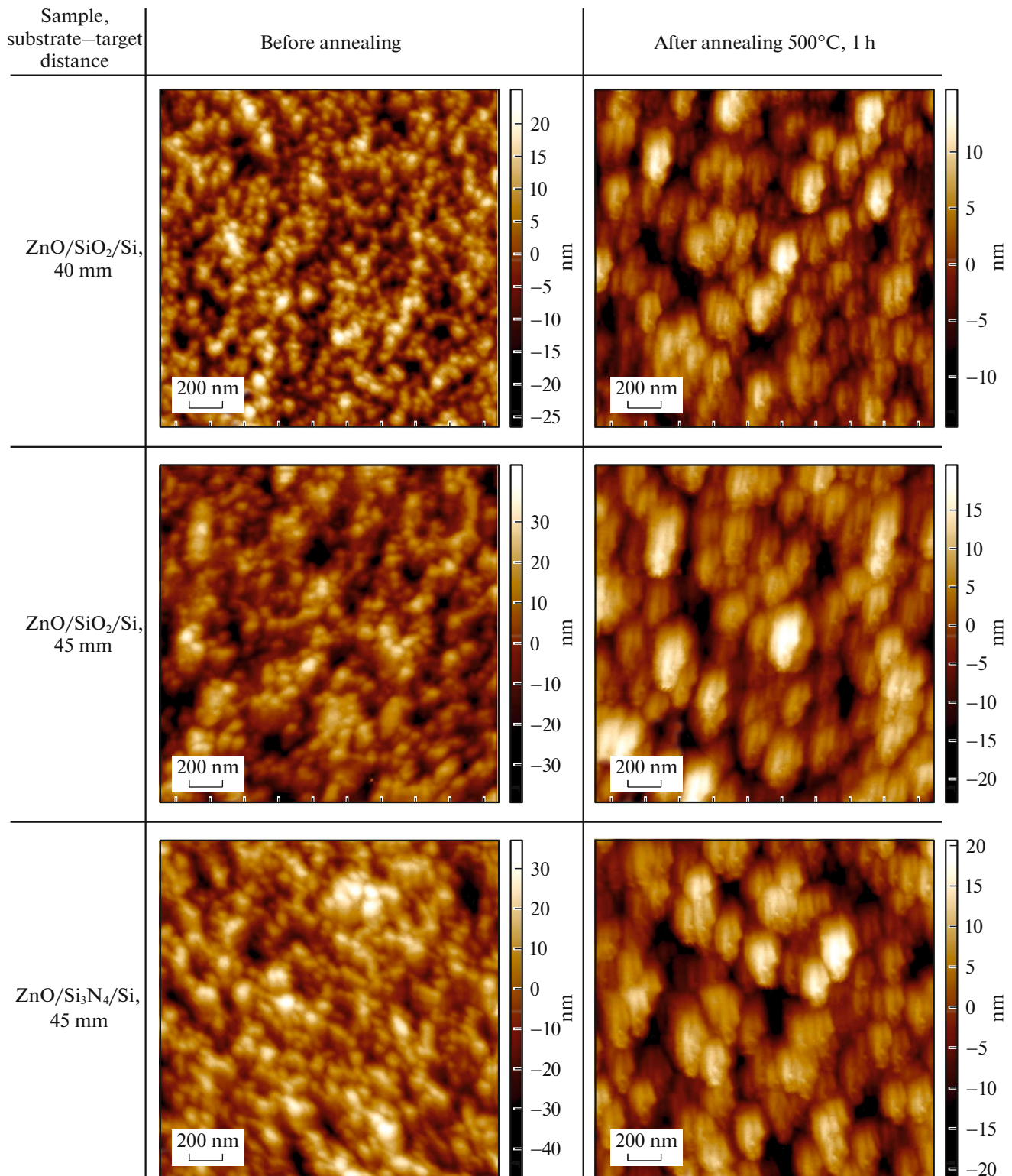**Fig. 4.** AFM images of the surfaces of ZnO films obtained at increased target−substrate distances.

XRDs. This result indicates that film crystallization occurs directly during its deposition. However, it should be noted that the shape of the peak changes significantly during annealing from 200°C. A decrease in the peak width may indicate the recrystallization process and an accompanying improvement in the crystallographic texture. It is important that after annealing, no additional ZnO reflections appear that indi-
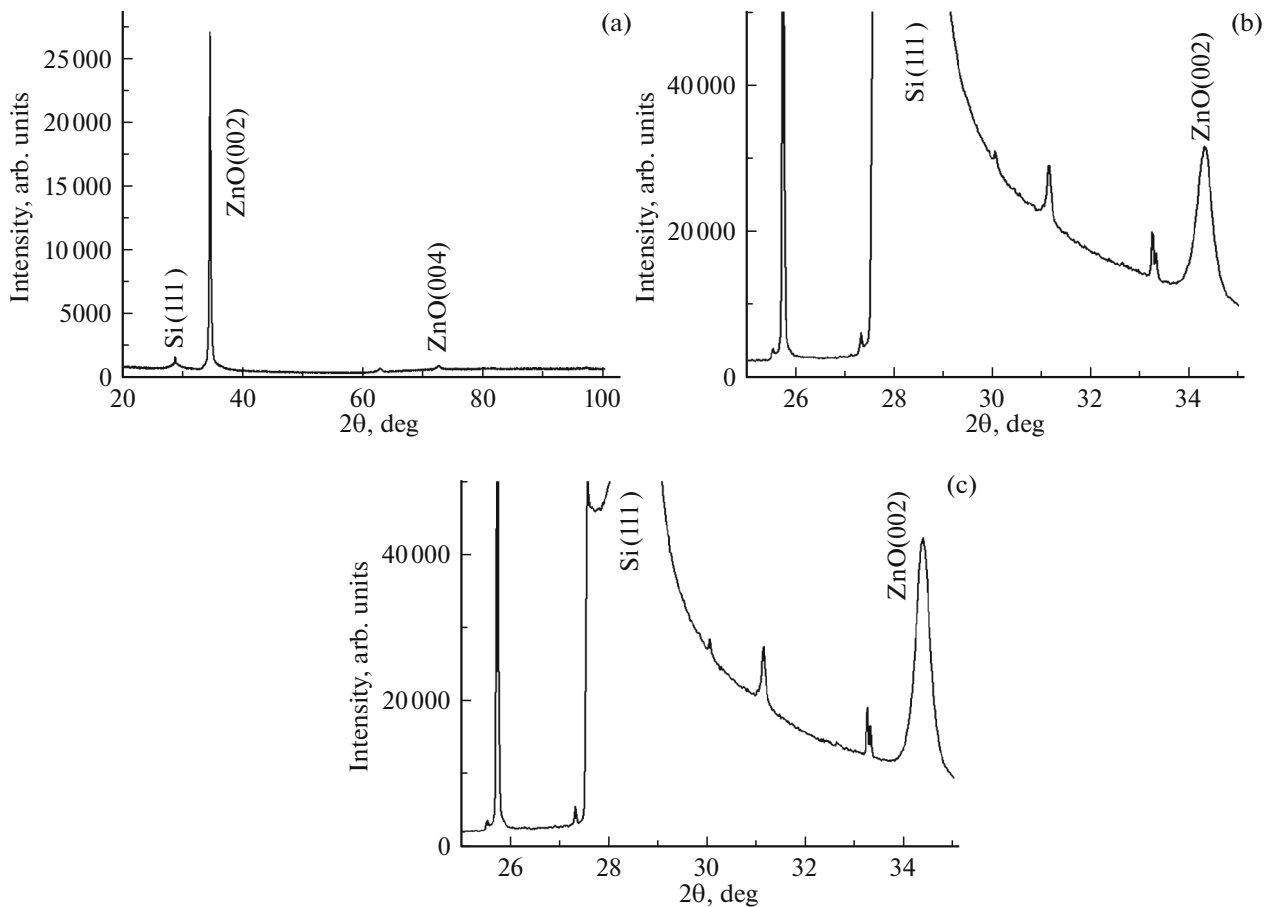
Fig. 5. X-ray diffraction patterns of ZnO films obtained at increased target–substrate distances (measurements before annealing): (a) ZnO/Si$_3$N$_4$/Si, 45 mm; (b) ZnO/SiO$_2$/Si, 40 mm; and (c) ZnO/SiO$_2$/Si, 45 mm.

cate the formation of a significant number of grains of another crystallographic orientation.

Figure 2 shows the evolution of the surface topography of the obtained ZnO films during annealing up to 500°C. In general, the AFM results are in good agreement with the diffraction-analysis data. Thus, all films, including those not subjected to heat treatment, show rounded grains that are characteristic of the (001) texture [16, 17], which confirms the formation of the ZnO crystal phase during the deposition process. Annealing at 100°C does not lead to noticeable transformations of the microstructure, and all significant changes occur at higher temperatures. After annealing at 200 and 350°C, rather large (~1 μm) inclusions that lead to a sharp increase in the roughness appear in the films. It can be seen that these inclusions are agglomerations of small grains with poorly distinguished boundaries. At the same time, after annealing at 500°C, no such formations are observed, and the surface topography is more similar to a film that has not been subjected to heat treatment. However, the grain size of a sample that was annealed at 500°C is on average larger than that of an unannealed film.

From the results obtained, we can clearly conclude that during annealing at 200°C (as well as at 350°C), ZnO recrystallization occurs locally. In other words, the growth and agglomeration of some crystallites requires a significantly lower energy than others. This "inhomogeneity" can be explained by different orientations of grains relative to one another in the [hk0]-type directions. In the plane of an amorphous substrate, it is rather difficult to distinguish any direction that is preferred for growth. In this regard, the (hk0) planes of crystallites that are perpendicular to the film surface can be oriented in an arbitrary manner. Because of this, the value of the angle between the (hk0) planes of two adjacent grains may differ for different pairs of crystallites (Fig. 3). The coalescence of contiguous grains occurs easier with a decrease in the angle of disorientation between the boundary planes. In this regard, at relatively low temperatures, the growth and agglomeration of crystallites that are disoriented only by relatively small angles can be observed. Apparently, when the annealing temperature increases to 500°C, this limitation for ZnO is removed and recrystallization occurs uniformly over the entire volume.

Table 1. Surface roughness of ZnO films obtained at increased target−substrate distances

Sample	Target−substrate distance, mm	Roughness, nm	Roughness after annealing at 500°C, nm
ZnO/SiO$_2$/Si	40	7.57	4.66
ZnO/SiO$_2$/Si	45	11.35	6.97
ZnO/Si$_3$N$_4$/Si	45	11.28	6.61

It was impossible to find similar results in publications due to the small number of such studies. Nevertheless, the study [18] can be considered close to this one in terms of the arrangement of the experiment. In this study, amorphous ZnO films were annealed for 1 h at temperatures of 200, 400, 600, and 800°C. In this case, there was no pronounced heterogeneity in the size of crystallites. This discrepancy with the results of this study can be explained by the fact that the growth of grains with an increase in the annealing temperature in [18] occurs due to more intense transformation of the amorphous phase, rather than due to the coalescence of grains. It follows from this fact that the film microstructure depends not only on the annealing temperature, but also on the initial state of the material.

From the results obtained, it can be concluded that the most optimal annealing temperature for ZnO is 500°C, at which recrystallization occurs throughout the entire film volume and no significant relief inhomogeneities occur. On the other hand, such annealing did not lead to a significant change in the roughness that was observed in other studies [19]. For an unannealed film, as well as for a sample with an annealing temperature of 500°C, the inhomogeneity over the relief (the root-mean-square roughness parameter) was ~13 nm. To reduce this value as a result of annealing, it is necessary to enhance the recrystallization process. On the one hand, this can be achieved by increasing the temperature; however, a similar effect must manifest itself if the film is initially characterized by better crystallinity. This approach was implemented in a series of experiments with an increased distance between the substrate and target.

It is known that when ions collide with a target, their reflection is possible, including elastic reflection [20]. Reflected ions may be incident on the substrate and create defects in the film. On the one hand, this leads to an increase in the number of crystallization centers. On the other hand, the crystal structure is violated, as a result of which the recrystallization processes slow down during annealing.

The defect-formation intensity can be reduced via an increase in the distance between the target and substrate; as a result, the energy of reflected ions decreases due to an increase in the number of collisions with atoms of the working and residual gases, as well as with sputtered particles themselves. However, the deposition rate decreases with this configuration; therefore, the process duration must be correspond-

ingly increased. On the other hand, a decrease in the rate itself can also promote a reduction in the number of defects. In addition to a change in the distance, ZnO was sputtered on Si$_3$N$_4$ (amorphous)/Si for better demonstration of the formation of the (001) texture by means of XRD, i.e., without unnecessary peaks from silicon oxide. The silicon-nitride film had a thickness of 50 nm and was obtained by plasma-chemical deposition on a Si (111) substrate. In an experiment with a target−substrate distance of 45 mm, sputtering on Si$_3$N$_4$/Si and SiO$_2$/Si substrates was performed simultaneously for correct comparison of the results. To maintain the order of the experiment, AFM research of samples was conducted immediately after film deposition, and also after annealing at 500°C as the most optimal temperature (Fig. 4). The surface morphology of the obtained films before annealing does not fundamentally differ from the initial samples. However, the ZnO reflections in XRDs can be characterized as much more pronounced, thus indicating a higher crystallinity of films (Figs. 5a, 5b). The changes that occurred in these films after annealing at 500°C are much more significant than when annealing a sample with a target−substrate distance of 25 mm at the same temperature. Thus, all grains increased by more than 2 times (Fig. 4), and the surface roughness decreased by ~40% (see Table 1).

Thus, this study demonstrates how the microstructural characteristics (grain size, roughness) of ZnO films depend on the annealing temperature and the initial state of samples. The samples that were obtained at an increased target−substrate distance and annealed at 500°C appear to be the most suitable candidates for the role of buffer layers.

4. CONCLUSIONS

Confirming the results of available published data, ZnO films with the (001) texture were obtained by the method of the ion-beam sputtering of a target on substrates made of thermally oxidized silicon wafers with the (111) orientation.

It is shown that the surface microstructure of such ZnO films changes after annealing in air at a temperature due to recrystallization processes. In this case, the recrystallization is local in the temperature range from 200 to 350°C: the coalescence of a small number of grains located inhomogeneously over the surface is observed. After annealing at 500°C, the grains increase in size uniformly over the entire film surface.

The intensity of this growth depends on the initial state of the sample. If there are many defects formed as a result of the effect of ions of the working gas that are reflected from the target, the growth of grains after annealing is insignificant. As the deposition rate and intensity of ion bombardment decrease, the size of crystallites after their heat treatment increases by several times, while the surface roughness decreases by ~40%.

CONFLICT OF INTEREST

The authors state that they have no conflict of interest.

REFERENCES

1. T. V. Blank and Yu. A. Gol'dberg, Semiconductors **37**, 999 (2003).

2. M. Matsuoka and M. Naoe, IEEE Trans. Magn. **25**, 1474 (1985).

3. E. Lacroix, P. Gerard, G. Marest, and M. Dupuy, J. Appl. Phys. **69**, 4770 (1991).

4. A. M. Glezer and N. A. Shurygina, *Amorphous-Nanocrystalline Alloys* (Fizmatlit, Moscow, 2013) [in Russian].

5. M. N. Volochaev, Yu. E. Kalinin, M. A. Kashirin, V. A. Makagonov, S. Yu. Pankov, and V. V. Bassarab, Semiconductors **53**, 1465 (2019).

6. D. Mendil, F. Challali, T. Touam, A. Chelouche, A. H. Souici, S. Ouhenia, and D. Djouadi, J. Lumin. **215**, 116631 (2019).

7. P. C. Dorsey and C. Vittoria, J. Magn. Magn. Mater. **137**, 89 (1994).

8. W. Yang, J. Liu, M. Liu, Y. Liu, N. Wang, G. Shen, Z. Liu, X. He, C. Zhang, L. Hu, and Y. Fu, Superlatt. Microstruct. **136**, 106291 (2019).

9. W. Yang, J. Liu, Z. Guan, Z. Liu, B. Chen, L. Zhao, Y. Li, X. Cao, X. He, C. Zhang, Q. Zeng, and Y. Fu, Ceram. Int. **46**, 6605 (2020).

10. P. Murkute, H. Ghadi, S. Sreedhara, and S. Chakrabarti, Superlatt. Microstruct. **136**, 106310 (2019).

11. A. Kumar, M. Prasad, V. Janyani, and R. P. Yadav, J. Electron. Mater. **48**, 5693 (2019).

12. Kh. A. Abdullin, L. V. Gritsenko, S. E. Kumekov, A. A. Markhabaeva, and E. I. Terukov, Semiconductors **52**, 177 (2018).

13. V. V. Ratnikov, R. N. Kyutt, S. V. Ivanov, M. P. Shcheglov, and A. Baar, Semiconductors **44**, 251 (2010).

14. N. V. Rumak, V. V. Khatko, and V. N. Plotnikov, Phys. Status Solidi A **86**, 93 (1984).

15. X. Zhang, Y. Duan, X. Dai, T. Li, Y. Xia, P. Zheng, H. Li, and Y. Jiang, Appl. Surf. Sci. **504**, 144437 (2020).

16. A. A. Camacho-Berríosa, V. M. Pantojas, and W. Otano, Thin Solid Films **692**, 137641 (2019).

17. X. Zhang, P. Wang, X. Liu, W. Zhang, Y. Zhong, H. Zhao, S. Shi, S. Jin, and Y. W. R. Amarasinghe, Surf. Coat. Technol. **361**, 123 (2019).

18. J. Bruncko, A. Vincze, M. Netrvalova, P. Sutta, D. Hasko, and M. Michalka, Thin Solid Films **520**, 866 (2011).

19. V. A. Smirnov, R. V. Tominov, V. I. Avilov, N. I. Alyabieva, Z. E. Vakulov, E. G. Zamburg, D. A. Khakhulin, and O. A. Ageev, Semiconductors **53**, 72 (2019).

20. L. V. Kozhitov, S. G. Emel'yanov, V. G. Kosushkin, S. S. Strel'chenko, Yu. N. Parkhomenko, V. V. Kozlov, and S. L. Kozhitov, *Micro- and Nanoelectronic Materials Technology* (YuZGU, Kursk, 2012) [in Russian].

Translated by A. Seferov